LAWRENCE
LIVERMORE
NATIONAL
LABORATORY

LLNL-PROC-587362

Measurement and Modeling of the n=2-3 Emission of O VIII near 102 Å

E. Trabert, P. Beiersdorfer

October 3, 2012

Highly Charged Physics
Heidelberg, Germany
September 2, 2012 through September 7, 2012

Disclaimer

Measurement and modeling of the n=2-3 emission of O VIII near 102 Å

Elmar Träbert[1,2], Peter Beiersdorfer[1]

1 Physics Division, Lawrence Livermore National Laboratory, Livermore, CA 94550, U.S.A.

2 Astronomisches Institut, Fakultät für Physik und Astronomie, Ruhr-Universität Bochum, D-44780 Bochum, Germany

E-mail: traebert@astro.rub.de

Abstract. In observations of Capella, the XUV emission compared to the EUV emission significantly exceeds expectation from collisional-radiative spectral modeling. This discrepancy is presently undergoing experimental verification at an electron beam ion trap. An important step of the procedure is the relative efficiency calibration of spectroscopic detection equipment for EUV and XUV observations, for which we use the branching ratio of 1s-3p and 2s-3p transitions in the H-like spectrum O VIII. We present high-resolution measurements and associated modeling of the O VIII emission near 102 Å, which consists not only of the two 2s-3p transitions, but also of two 2p-3s and three 2p-3d transitions.

Submitted to: *Phys Scr T*

PACS numbers: 3230Rj; 3270Fw;

1. Introduction

Capella (α Aurigae) is one of the brightest objects in the Northern sky and has therefore most extensively been studied by using the high-resolution grating spectrographs onboard spacecrafts such as *Chandra* or *XMM/Newton*. Owing to the high data quality of the soft-x-ray (XUV) and extreme ultraviolet (EUV) spectra recorded, detail problems can be studied that in photon-starved observations cannot. One such problem is the finding [1] that the line ratio of XUV to EUV lines of Fe XVIII and Fe XIX is about a factor of three higher in the Capella data than is expected from spectral models based on codes such as APEC, even after correcting for the wavelength-dependent interstellar extinction. The reason may lie, of course, with the star, the modeling code, the assumed stellar parameters used in the model, absorption by the interstellar medium, or any combination thereof. The situation is further complicated by the fact that the bright object Capella actually consists of two giant stars of different temperature and luminosity that have been spatially resolved interferometrically, but are observed

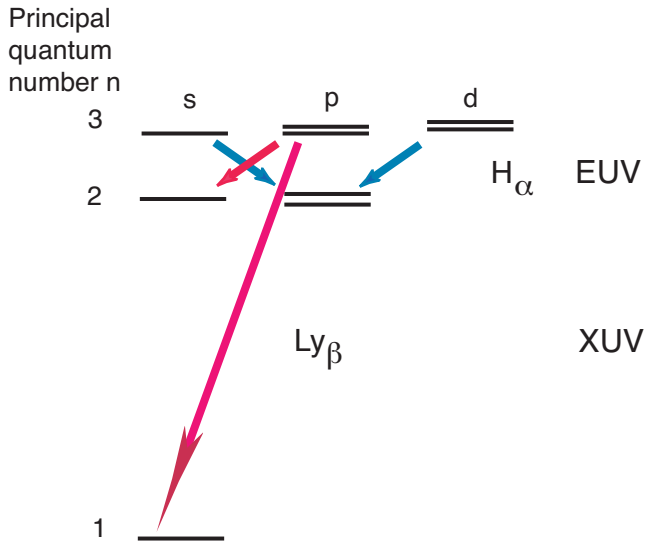

Figure 1. (Colour online) Schematics of 1-3 and 2-3 transitions in the H-like ion O^{7+}.

jointly with most other means. Any meaningful collisional-radiative model would have to present a superposition of the simulated spectra of the two stars. However, typical modeling efforts so far are based on the assumption that the EUV and XUV emission is dominated by the hotter of the two stars for which a temperature near 6 MK is generally assumed.

In a quest for experimental tests of the validity of such collisional-radiative models we have undertaken a study (with first results indicated elsewhere [2]) employing the Livermore electron beam ion trap (EBIT) [3, 4]. Among laboratory light sources, electron beam ion traps come closest to the conditions of a stellar coronal plasma [5], and they offer easy access for spectroscopy. Our aim is to compare the line ratios of the same XUV and EUV lines of Fe XVIII and Fe XIX as have been exploited by Desai *et al* for Capella [1]. The XUV lines fall into the range 13 to 18 Å, whereas the EUV lines of interest are to be found in the range 90 to 130 Å. Laboratory observations of the two ranges have to be put on a common footing in terms of detection efficiency. For this purpose we employ the decay branches of the 3p level of the hydrogen-like oxygen ion (spectrum O VIII, see Figure 1). The XUV branch is the Lyman-beta (Ly_β) line (transition 1s - 3p) at 16 Å, whereas the 2s - 3p transition is part of the Balmer-alpha (H_α) line at 102.4 Å. What fraction of the latter line actually represents the decay branch of interest may be estimated by spectral modeling using the FAC code [6]. We have also recorded high-resolution spectra of this line in order to ascertain that there are no line blends.

2. Experiment

The electron density in the stellar corona of Capella is estimated as 10^{10} cm^{-3}. Although it seems possible to operate the electron beam of an EBIT at such a low density, we work at somewhat higher electron densities (for the benefit of the signal-to-noise ratio) on the order of 1 to 5 $\times$ 10^{11} cm^{-3}, which ist still lower by two to three orders of magnitude than that of, for example, a tokamak plasma. The electron beam energy in relation to the ionization potential of subsequent ionization stages of the trapped ions that are hit by the electron beam dictates the highest charge state achievable. Iron ions Fe^{17+} and Fe^{18+} have been readily produced and the associated XUV and EUV lines dispersed and detected by two flat-field spectrometers (FFS) with variable spacing diffraction gratings and their microchannelplate (MCP) and cryogenic charge-coupled device (CCD) detectors, respectively. Although a smallish FFS of moderate resolving power (our SFFS instrument; grating 1200 ℓ/mm, R=5 m [7]) covered both aforementioned wavelength ranges at once, the detection efficiency in the XUV was rather low. Instead, a R=44.3 m instrument (our GFFS instrument; grating 2400 ℓ/mm [8]) was used for the XUV and also for separate detailed spectra near the O VIII H_α line (in the EUV).

Specimen spectra of Fe have been shown elsewhere [2]; here we concentrate on spectra of oxygen that serve to establish the relative detection efficiencies in the two observation ranges. Figure 1 illustrates the underlying idea. One-electron ions (such as O^{7+}) are considered to be well calculable. Hence quantum mechanics can readily yield the branching ratio of the 1s-3p and 2s-3p transitions (7.45:1). This value is independent of any plasma condition, since the same upper level is available for both decay branches. Oxygen is fed to EBIT as CO_2 in a continuous stream at ultrahigh vacuum (UHV) conditions. The energetic electron beam easily fragments any molecules it hits and ionizes the radicals. Figure 2 shows an XUV spectrum of oxygen with the Ly_β line (1s - 3p) at 16 Å; figure 3 displays the EUV spectrum of oxygen with the relatively weak H_α line at 102.4 Å.

Owing to the small fine structure intervals in H-like atoms and ions and the practical degeneracy of levels with a given total angular momentum value j, the H_α line represents a transition multiplet that consists not only of the two 2s-3p transitions, but also of two 2p-3s and three 2p-3d transitions. The wavelengths of the fine structure components are known from accurate calculations [9]. The relative populations of all the levels involved depend on the plasma conditions, and collisional-radiative modeling is required to find out which fraction of the total line intensity is expected to originate from the 2s-3p transitions of interest for the calibration. H_α appears broader than other lines even in the moderate-resolution spectrum of figure 3. Employing the GFFS spectrograph with its superior resolving power, the spectrum in figure 4 (recorded at an electron beam energy of 3 keV) shows a 'magnification' of the wavelength range 91 to 107 Å, with a spectral series (O VI 2s-np) for wavelength reference. In another magnification step, part of the same spectrum is displayed in figure 5, clearly showing a split of the H_α line

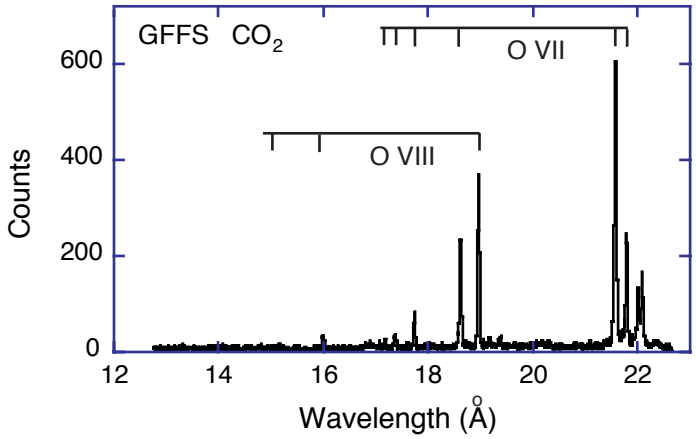

Figure 2. Spectrum of oxygen in the range 13 to 22 Å recorded with the GFFS spectrograph, also indicating the O VII $1s^2$ - 1snp and O VIII 1s - np line series. The spectrum was recorded at an electron beam energy of 6 keV.

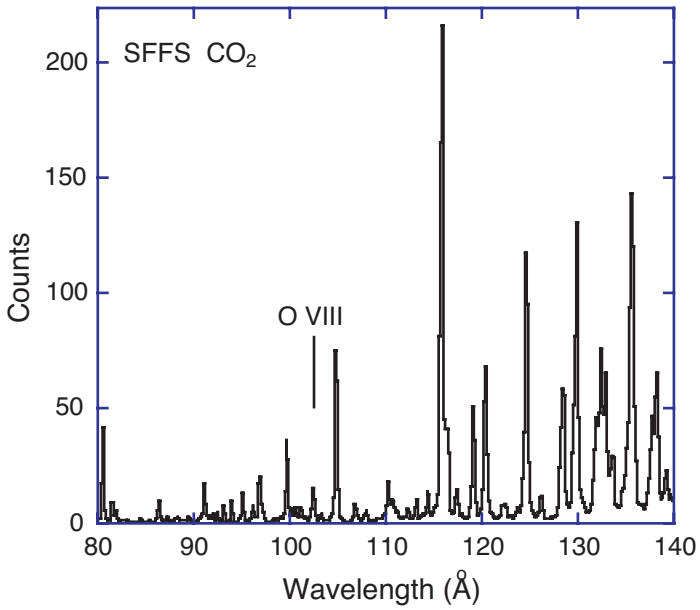

Figure 3. Spectrum of oxygen in the range 80 to 140 Å recorded with the SFFS spectrograph. The spectrum was recorded at an electron beam energy of 6 keV. The unlabeled lines are mostly from O VII, O VI, and O V.

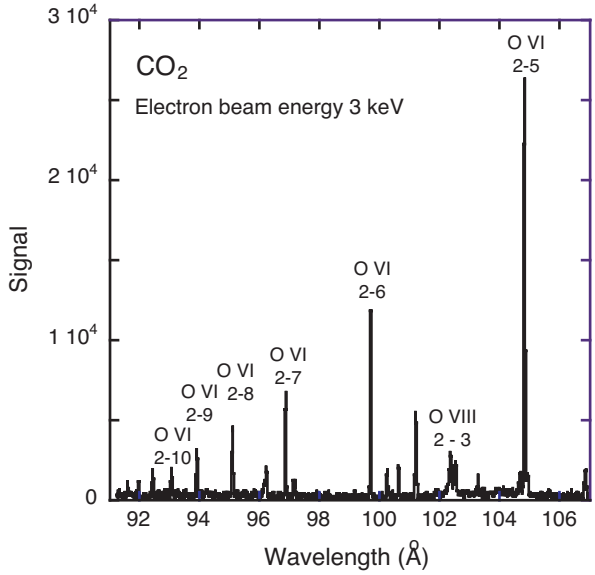

Figure 4. Spectrum of oxygen in the range 91 to 107 Å recorded with the GFFS spectrograph. The spectrum was recorded at an electron beam energy of 3 keV.

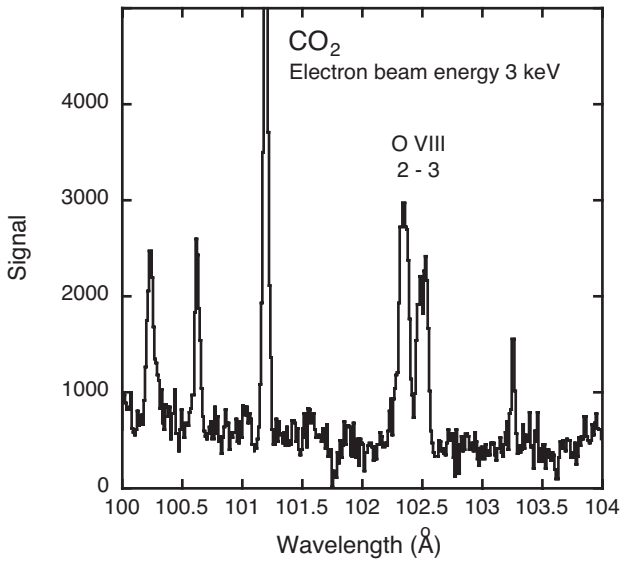

Figure 5. Section of the spectrum of oxygen of figure 4 in the vicinity of the O VIII 102.4 Å line.

into two major components (reflecting the fine structure splitting of the 2p levels) and some substructure.

Figure 6 indicates the relative intensities of the seven components of H_α that a collisional-radiative model based on FAC predicts, and an envelope of the multiplet derived from the components and an assumed line width close to our observations which employ a spectral resolving power of about 2000. There is reasonable overall agreement in the relative intensities of the two major line groups and their wavelength splitting

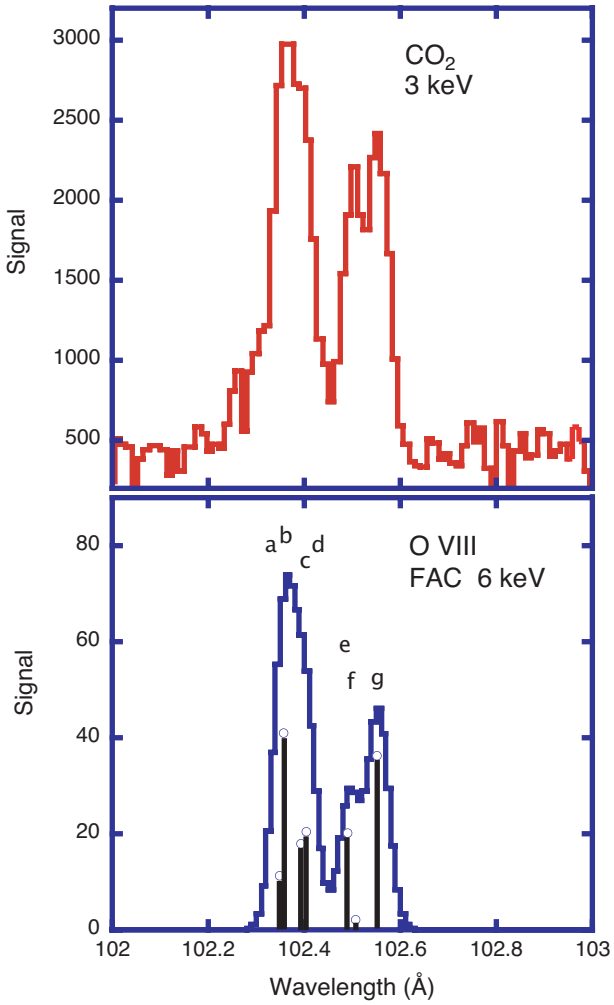

Figure 6. (Colour online) Top: O VIII H_α line profile measured at an electron beam energy of 3 keV. Bottom: Relative line intensities of the seven components of the O VIII 102.4 Å line predicted by FAC and simulated line envelope for excitation at 6 keV. The seven multiplet components are a) $2p_{1/2}$-$3d_{3/2}$, b) $2s_{1/2}$-$3p_{3/2}$, c) $2p_{1/2}$-$3s_{1/2}$, d) $2s_{1/2}$-$3p_{1/2}$, e) $2p_{3/2}$-$3d_{5/2}$, f) $2p_{3/2}$-$3d_{3/2}$, and g) $2p_{3/2}$-$3s_{1/2}$.

with the observed line profile; hence we can exclude that any notable spectral blends with unwanted lines are present.

Figure 7 shows synthetic profiles of the O VIII H_α line modeled for electron beam energies 3 keV (as in the present oxygen measurement) and 6 keV (as in our study of the Capella spectra), respectively. Evidently the long-wavelength component is expected to decrease with a higher electron beam energy, reflecting an energy-dependent change in the population of n=3 fine structure levels. Our FAC calculations show almost no dependence on the relative line intensities within the H_α feature as a function of electron density when varying the latter from 5 $\times 10^{10}$ cm^{-3} to 5 $\times 10^{12}$ cm^{-3}, but the relative intensities of 3s and 3d level decays decrease and of 3p increase with increasing electron beam energy. However, these changes are small compared to a major difference in detail,

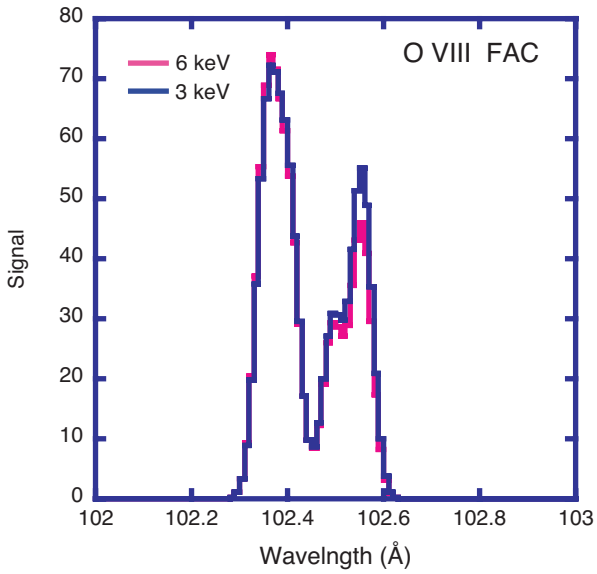

Figure 7. (Colour online) FAC simulations of the O VIII 102.4 Å line structure for electron beam energies of 6 keV (full red line) and 3 keV (blue line).

which is most clearly apparent on the short-wavelength side of the long-wavelength peak. That is the position of the $2p_{3/2}$ - $3d_{5/2}$ component, and it appears significantly (50%) stronger in the experiment than in the FAC model. The weaker $2p_{1/2,3/2}$ - $3d_{3/2}$ component is part of the unresolved blend that makes up the short-wavelength peak. If we assume a similar correction for the $3d_{3/2}$ level population, we have to balance this by reducing the weaker $2p_{1/2}$ level population in order to achieve an overall pretty good agreement of (adjusted) model prediction (see figure 8) and observed H_α line profile.

If the 2p-3d components are underpredicted and the model adjusted correspondingly (see figure 8), then the fraction of 2s-3p transitions contributing to H_α has to be lowered from the original FAC prediction (0.41 for an electron beam energy of 6 keV). The changes demonstrated in figure 8 imply a reduction of the fraction from 0.36 (at 3 keV) to about 0.25.

Of course, there is an alternative to the underprediction stated, a blend with a weak line of unknown origin in the same location as the $2p_{3/2}$ - $3d_{5/2}$ component of O VIII H_α. Such a blend with an unknown line of a few-electron ion of another ion species is not likely, since we see no other indication for correspondingly intense foreign contaminants.

Combining the effect of the 30% underprediction with a $\pm$10% variation of the predicted fraction that the 2s-3p line emissivities have of the total H_α line emissivity under a sensible variation of parameters, we deduce an uncertainty on the order of 15% for the key number of our calibration exercise, that is, the use of the O VIII 1s-3p/2s-3p branching ratio in establishing the relative detection efficiencies in the XUV vs. the EUV range.

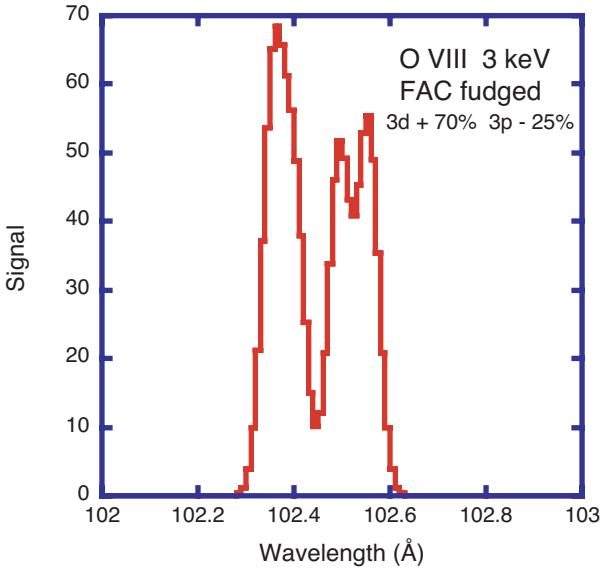

Figure 8. (Colour online) FAC simulations of the O VIII 102.4 Å line structure for an electron beam energy of 3 keV. The level populations predicted by FAC have been increased by 60% for the 3d levels and reduced by 30% for the 3p levels. This improves the match with the experimental line profile considerably (figure 5).

3. Discussion

The actual calibration for the Fe XVII and Fe XIX line ratio evaluation combines a measurement of the O VIII 1s-3p line in the XUV using the GFFS spectrograph with a measurement of the O VIII 2s-3p line in the EUV using the SFFS spectrograph which has a lower resolving power. The 1s - np XUV line series in comparison with FAC modeling helps to verify that in the interplay of decreasing diffraction/reflection efficiency of the grating towards shorter wavelengths and the increasing efficiency of the MCP detector the overall detection efficiency is rather flat over the range of interest for the Fe XVIII/Fe XIX measurements. Moreover, the same line series helps to estimate the Ly$_\beta$ line intensity from the unblended other lines of the same series when Ly$_\beta$ itself is blended with iron lines. (Oxygen is part of the ironpentacarbonyl molecule we employ to introduce Fe into EBIT.)

Considering the EUV decay branch, the SFFS measurements produce a line that is somewhat broader than the other oxygen lines in the spectrum, suggesting the possible occurrence of a line blend. Our high-resolution measurements now demonstrate that the broadening is not due to a blend (although an unidentified weak line appears on the short-wavelength shoulder of the spectral feature)), but to the fine structure of the H$_\alpha$ line. The integrated signal over this line thus has to take the fine-structure broadening into account. Moreover, the high spectral resolution reveals decay components associated with individual n=3 fine structure levels and allows us to adjust the FAC predictions to experimental observation. This correction will significantly

reduce the inconsistency that arises between EBIT XUV and EUV data compared to FAC modeling predictions without this insight. The new data yield an error estimate on some aspects of modeling by FAC that are important for the application of the Ly_β / H_α line ratio as a XUV/EUV calibration reference. However, one has to be aware of the complication possibly caused by polarization of the decays of levels with j>1/2. The main effect of the linear polarization of lines by a directional electron beam in this case will be the angular distribution, which for an E1 line at 90° to the beam produces an enhancement by a factor of 3/(3-P), where P is the polarization [10]. Assuming P being possibly as high as 0.5 (the polarization of the Ly_α line is less than this value [11]), the effect would be a $< 20\%$ enhancement for the lines emanating from the $3p_{3/2}$, $3d_{5/2}$, or $3d_{3/2}$ levels.

The O VIII H_α line has previously been studied with similarly high spectral resolution, but at a different light source [12]. Müller *et al* observed a foil-excited fast ion beam, controlling the Doppler broadening of the line of interest by inserting an auxiliary slit to drastically reduce the solid angle of acceptance of their grazing-incidence spectrometer. Their H_α line profile looks significantly different from ours, for several reasons. The observation of a fast ion beam through a narrow aperture implies time resolution on the order of a few picoseconds, which reduces the contribution seen from the 3s level decay (predicted lifetime 39 ps) and favours the observation of the much shorter-lived 3d level decay (calculated lifetime 0.4 ps). Moreover, in the ion-foil interaction process, the excitation is non-selective and thus close to statistical, or proportional to the statistical weight $2\ell+1$, which leads to a prominent cascade chain feeding the very 3d levels. In contrast, our measurement records time-integrated data under quasi-steady state conditions and thus without weighting by level lifetime. In addition, our data and FAC indicate a much smaller contribution of 3d level decays to our line pattern compared to a statistical level population, because direct excitation from the 1s ground state disfavours the population of levels with angular momentum $\ell > 1$.

Acknowledgments

This work was performed under the auspices of the U.S. Department of Energy by Lawrence Livermore National Laboratory under Contract DE-AC52-07NA27344 and was supported by NASA grant NNH07AF81I. E.T. acknowledges support from the German Research Association (DFG) grant Tr171/18.

References

[1] Desai P, Brickhouse N, Drake J J, Dupree A K, Edgar R J, Hoogerwerf R, Kashyap V, Wargelin B J, Smith R K, Huenemoerder D P, Liedahl D A 2005 *Astrophys. J.* **625** L59

[2] Träbert E, Beiersdorfer P, Clementson J 2012 *AIP Conf. Proc.* **1438** 142

[3] Levine M A, Marrs R E, Henderson J R, Knapp D A, Schneider M B 1988 *Phys. Scr.* T**22** 157

[4] Levine M A, Marrs R E, Bardsley J N, Beiersdorfer P, Bennett C L, Chen M H, Cowan T, Dietrich D, Henderson J R, Knapp D A, Osterheld A L, Penetrante B M, Schneider M B, Scofield J H 1989 *Nucl. Instrum. Meth. Phys. Res.* B**43** 431
[5] Beiersdorfer P 2003 *Ann. Rev. Astron. Astrophys.* **41** 343
[6] Gu M-F 2008 *Can. J. Phys.* **86** 675
[7] Beiersdorfer P, Crespo López-Urrutia J R, Springer P, Utter S B, Wong K L, 1999 *Rev. Sci. Instrum.* **70** 276
[8] Beiersdorfer P, Magee E W, Träbert E, Chen H, Lepson J K, Gu M-F, Schmidt M 2004 *Rev. Sci. Instrum.* **75** 3723
[9] Garcia J D, Mack J E 1965 *J. Opt. Soc. Am.* **55** 654
[10] Beiersdorfer P, Vogel D A, Reed K J, Decaux V, Scofield J, Widmann K, Hölzer G, Förster E, Wehrhan O, Savin D W, Schweikhard L 1996 *Phys. Rev.* A **53** 3974
[11] Robbins D L, Beiersdorfer P, Faenov A Ya, Pikuz T A, Thorn D B, Chen H, Reed K J, Smith A J, Brown G V, Kelley R L, Kilbourne C A, Porter F S 2006 *Phys. Rev.* A **74** 022713
[12] Müller H R, Heckmann P H, Träbert E 1982 *Z. Physik* A**308** 283